Photophysical Properties of Quinolizinium Salts and Their Interactions with DNA in Aqueous Solution†

Arianna Barbafina, Matteo Amelia, Loredana Latterini, Gian Gaetano Aloisi, and Fausto Elisei*

Dipartimento di Chimica and Centro di Eccellenza sui Materiali Innovativi Nanostrutturati (CEMIN), via Elce di Sotto 8, Perugia 06123, Italy

Received: April 30, 2009; Revised Manuscript Received: May 28, 2009

The photophysical properties of three quinolizinium salts (naphto[2,1-*b*]quinolizinium bromide (Q2), naphto[1,2-*b*]quinolizinium bromide (Q3), and indolo[2,3-*b*]quinolizinium tetrafluoroborate (HI)) in fluid media and their interactions with DNA were investigated by steady-state and by nanosecond and femtosecond time-resolved techniques. The main decay pathways of the excited singlet state S_1, fluorescence, intersystem crossing, and internal conversion, were characterized in terms of quantum yields and rate constants. The lowest triplet state of the quinolizinium salts is able to sensitize singlet oxygen in rather high efficiency ($\phi_\Delta = 0.4$ to 0.5 in MeCN). The complexes between quinolizinium salts and DNA formed in the ground state were characterized in terms of lifetimes and decay channels to give more details of the mechanism of photoinduced DNA strand break.

Introduction

Increasing interest has been devoted in the last several years to quinolizinium salts, cationic aromatic dyes that are able to bind efficiently to DNA and cause photoinduced DNA cleavage.[1−6]

This photobiological activity, photonuclease, can produce intentional DNA photodamages, for example, in tumor cells; therefore, these dyes may have applications in photochemotherapy.[7,8] Recently, investigations of DNA-binding and DNA-photodamaging properties of indolo[2,3-*b*]quinolizinium bromide were reported.[1,2,4] Analysis of the association constants with different polynucleotides revealed that indolo[2,3-*b*]quinolizinium bromide binds preferentially to GC base pairs and moreover that irradiation of DNA in the presence of this dye caused an efficient single-strand cleavage of the nucleic acid.[1,2,4]

Spectrophotometric and spectrofluorimetric measurements showed that naphtoquinolizinium cations bind to DNA by intercalation with a binding constant (K_a) of about 10^5 M^{-1}, and the highest affinity was observed for GC base pairs.[3] Moreover, efficient DNA damage was observed upon UV-A irradiation in the presence of naphtoquinolizinium salts. The preliminary analysis indicated that the photocleavage takes place preferentially at the guanine-rich region.[5] However, little is known about the mechanism of DNA photocleavage sensitized by quinolizinium salts. Few indirect experiments on similar compounds[9] indicate that reactive oxygen intermediates are involved in DNA photocleavage.

Experiments also revealed that the major pathways in the acridizinium-induced DNA damage occur via the formation of hydroxyl radicals or singlet oxygen. The mechanism proposed also provided evidence that the DNA-bound acridizinium complex does not form the excited triplet state upon irradiation.[9]

This work is aimed at producing a detailed photophysical characterization of four-ring quinolizinium salts (indolo[2,3-*b*]quinolizinium tetraborate, HI; naphto[2,1-*b*] quinolizinium bromide, Q2; naphto[1,2-*b*]quinolizinium bromide, Q3) and their complexes with DNA to obtain direct evidence of DNA−quinolizinium salt interactions.

The S_1 state of the compounds under investigation was characterized by fluorescence techniques, and the spectroscopic and kinetic properties of the triplet state were determined by laser flash photolysis. The efficiency of singlet oxygen sensitization was quantified by recording the emission intensity of $O_2(^1\Delta_g)$ centered at 1270 nm.

The effect of DNA on the decay pathways of the lowest excited singlet and triplet states of Q2, Q3, and HI in aqueous buffer at pH 7.2 was investigated by fluorescence and flash photolysis measurements. The ultrafast absorption behavior of Q2 and Q3 was investigated by 40 fs excitation to better elucidate the dynamics of the DNA−substrate complexes.

Experimental Section

Chemicals. The quinolizinium salts naphto[2,1-*b*]-quinolizinium bromide (Q2), naphto[1,2-*b*]quinolizinium bromide (Q3), and indolo[2,3-*b*]quinolizinium tetrafluoro-borate (HI) were kind gifts of Dr. G. Viola (Padua, Italy). Benzophenone (Aldrich, gold label) was used as received. Disodium 3,3′-disulfonatobenzophenone was that used in a previous work.[10] Salmon testes DNA (sodium salt) was from Sigma Co. (St. Louis, MO). Base pair concentrations were determined spectrophotometrically using the value of 13 200 M^{-1} cm^{-1} for the molar absorption coefficient at 260 nm. Acetonitrile (Fluka, spectrophotometric grade) was used as received. The pH of aqueous solutions (pH = 7.2) was adjusted by ETN buffer (10 mM TRIS, 1 mM EDTA, and 10 mM NaCl).

Absorption and Fluorescence. Absorption spectra were recorded with a Perkin-Elmer Lambda 800 spectrophotometer. Fluorescence spectra and quantum yields were measured with a Fluorolog-2 (Spex, F112AI) spectrophotofluorimeter (mean deviation of three independent experiments, ca. 5% for ϕ_F) in solutions air-equilibrated (absorbance <0.1 at the excitation

† Part of the "Vincenzo Aquilanti Festschrift".

* Corresponding author. Fax: +39-075-5855598. Tel: +39-075-5855588. E-mail: elisei@unipg.it.

10.1021/jp9040315
Published on Web 07/22/2009

wavelength) by using anthracene in ethanol as standard, $\phi_F = 0.27$.[11] The fluorescence lifetimes, τ_F (mean deviation of three independent measurements, ca. 5%), were measured by a Spex Fluorolog-τ2 system, which uses the phase-modulation technique (excitation wavelength modulated in the 1−300 MHz range; time resolution ca. 10 ps). The frequency-domain intensity decays (phase angle and modulation vs frequency) were analyzed with the Global Unlimited (rev.3) global analysis software.[12] The τ_F values in the presence of increasing DNA concentrations were measured by use of an Edinburgh Instruments 199S spectrofluorimeter with the single photon counting method using a hydrogen-filled lamp.

Laser-Flash Photolysis. Triplet states formation quantum yields and lifetimes were measured with a flash photolysis setup previously described (Nd/YAG Continuum, Surelite II, third harmonics, $\lambda_{exc} = 355$ nm, pulse width ca. 7 ns and energy ≤ 1 mJ pulse^{-1}).[13,14] First-order kinetics were observed for the decay of the lowest triplet state. (T-T annihilation was prevented by the low excitation energy.) The triplet lifetimes were measured at an absorbance of ca. 0.4. The concentration effect on the triplet lifetime was not investigated. We obtained the transient spectra by monitoring the change in absorbance at intervals of 10 nm over the 300−740 nm range and averaging at least 10 decays at each wavelength. The calibration of the experimental setup was made with an optically matched acetonitrile solution of benzophenone ($\phi_T = 1$ and $\Delta\varepsilon_T = 6500$ M^{-1} cm^{-1} at the corresponding absorption maximum).[15] The $\Delta\varepsilon_T$ (and then ϕ_T) values were determined by the energy transfer method by the use of benzophenone and disodium 3,3′-disulfonato-benzophenone as donors in MeCN and ETN buffer, respectively; for the latter, the same triplet properties of benzophenone were assumed.[16] We obtained the product $\varepsilon_T \times \phi_T$ for each compound by comparing the change of absorbance of optical matched solutions of the substrate and the standard. All measurements were carried out at 22 ± 2 °C. The solutions were saturated by bubbling with nitrogen. The experimental errors on τ_T were estimated to be about ±10 and ±15% for $\Delta\varepsilon_{T\text{-}S}$ and ϕ_T. The photostability of the compounds under investigation was further proven by the spectrophotometric analysis before and after the flash photolysis measurements.

Singlet Oxygen. We determined the singlet oxygen quantum yields (ϕ_Δ) by recording the phosphorescence intensity of $O_2(^1\Delta_g)$ with a germanium diode detector in air-equilibrated MeCN solutions.[17,18] The amplified signal extrapolated at zero time was plotted as a function of the laser dose. Linear relationships were obtained for Q2, Q3, and HI and for phenalenone used as standard ($\phi_\Delta = 0.97 \pm 0.03$).[19] The ϕ_Δ values were then obtained from the ratio of the slopes of the substrate to that of phenalenone multiplied by the known ϕ_Δ of the standard. At least 200 kinetics were averaged for each solution. The experimental error of ϕ_Δ was estimated to be about ±15%.

Time-Resolved Femtosecond Absorption and Emission. Femtosecond (fs) pulses were generated by an amplified titanium−sapphire laser system (Spectra Physics, Mountain View, CA) that produces 1 W pulses of 40 fs centered at 800 nm with a repetition rate of 1 kHz. Pump pulses centered at 400 were obtained by second harmonic generation in a 500 μm β-barium-borate crystal. In the transient absorption set up (Helios, Ultrafast Systems), the pump pulses were passed through a chopper that cut out every second pulse and collimated to the sample in a 2 mm quartz cuvette. We produced probe pulses for optical measurements by passing a small portion of 800 nm light through an optical delay line (with a time window of 1600 ps) and focusing into a 2 mm thick sapphire crystal to generate a white-light continuum in the 450−800 nm window. The white light was focused onto the sample, and we determined the chirp inside the sample cell by measuring the laser-induced Kerr signal of the solvent.

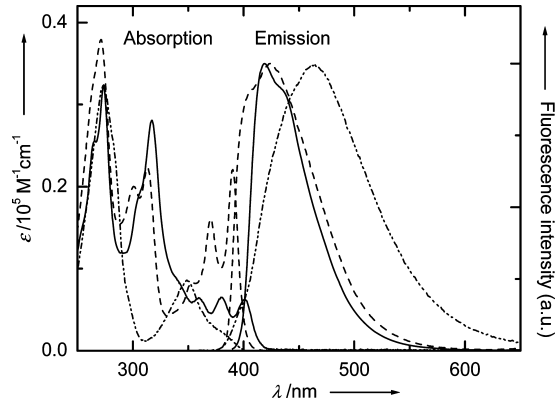

Figure 1. Absorption and normalized emission spectra of Q2 (solid), Q3 (dash), and HI (dot) in aqueous ETN buffer (pH = 7.2).

The used femtosecond time-resolved fluorescence spectroscopy employs the upconversion technique (Halcyone, Ultrafast Systems). The femtosecond laser pulses are generated by a mode-locked Ti−sapphire laser pumped by a frequency doubled Nd/YVO_4 continuous wave laser (Tsunami, Millennia Vs, Spectra Physics). The laser pulses, not amplified, have a wavelength of 800 nm, whereas their pulse duration and repetition rate are 80 fs and 82 MHz, respectively. The laser beam is focused onto a nonlinear BBO crystal (1 mm thickness) generating a second harmonic beam at 400 nm. The two beams (fundamental and second harmonics) are separated through a prism. The second harmonic (6 mW average power), after passing through a half wave plate, excites the sample contained in a 2 mm thick quartz cuvette. The remaining fundamental laser beam plays the role of the "optical gate" after passing through an optical delay line with a time window of 3200 ps. The fluorescence of the sample is collected and focused onto a second BBO crystal (1.5 mm thickness) together with the delayed fundamental laser beam. The upconversion beam is focused by a lens into the entrance of a monochromator, and it is finally detected by a photomultiplier connected to a photon counter having an exposure time equal to 1 s at each delay point. The temporal resolution of our time-resolved spectroscopic technique is about 150 fs, whereas the spectral resolution is 2.5 nm.

The measurements were carried out under magic angle to avoid the influence of the rotational diffusion in a 2 mm cell and at an absorbance of about 0.8 at 400 nm, except where otherwise mentioned.

Results and Discussion

Absorption and Emission Spectra. The absorption spectra of Q2, Q3, and HI were recorded in acetonitrile and aqueous ETN buffer at pH 7.2. In general, the spectra show three bands in the range of 250−450 nm. (See Figure 1 as an example.) In agreement with a vibrational mode due to the stretching C−C of aromatic rings,[20] a vibrational structure with a step of ca. 1420 and 1360 cm^{-1} for Q2 for Q3, respectively, was also detected. Moreover, the spectra of Q2 and Q3 do not significantly change with the solvent, the pH of the medium, and the ground-state concentration (in the 10^{-4} to 10^{-5} M range). This behavior means that the energy and nature of the singlet states

TABLE 1: Fluorescence Properties and Decay Rate Constants of the Lowest Singlet State of Q2, Q3, and HI

	solv.	λ_{em}/nm	ϕ_F	τ_F/ns	$k_F/10^7$ s^{-1}	ϕ_{IC}	$k_{IC}/10^7$ s^{-1}	$k_{ox}/10^{10}$ s^{-1}
Q2	MeCN	420	0.15	8.7	1.7	0.55	6.2	1.6
	ETN	419	0.18	7.8	2.3	0.46	5.9	
Q3	MeCN	425	0.34	5.6	6.1	0.23	4.1	1.7
	ETN	424	0.40	5.2	7.7	0.10	1.9	
HI	MeCN	457	0.17	10.5		0.46		2.0
	ETN	464	0.20	8.9	2.2	0.40	4.4	

The fluorescence lifetime values for HI are reported in Table 1, and they range from 8.9 to 10.5 ns and can be assigned to the aggregate species.

TABLE 2: Triplet Properties of Q2, Q3, and HI

	solv.	λ_{max}/nm	τ_T/μs	ϕ_T	$\Delta\varepsilon_T$/M^{-1} cm^{-1}[a]	$k_{ISC}/10^7$ s^{-1}	$k_{ox}/10^9$ M^{-1} s^{-1}	ϕ_Δ
Q2	MeCN	380, 460, 600	5.6	0.30	5400	3.4	1.5	0.40
	ETN	380, 410, 550	4.9	0.36	4400	4.6	1.2	
Q3	MeCN	340, 510	4.3	0.43	5800	7.7	1.5	0.46
	ETN	340, 410, 490	8.5	0.50	5800	9.6	2.3	
HI	MeCN	320, 400, 670	3.3	0.37	5100		1.3	0.48
	ETN	310, 380, 690	9.0	0.39	5100	4.6	1.8	

[a] Change of absorption coefficient measured at the underlined maximum.

of these substrates are fundamentally independent of the medium nature. The different spectral behavior of HI is due to the expansion of the indole π-conjugation, which shifts the fluorescence emission maximum at longer wavelengths and increases the Stokes shifts.[21] Furthermore, in the case of HI, the absorption spectrum was affected by the solvent and in organic media also by the ground-state concentration in the range of 10^{-4} to 10^{-5} M, so aggregate formation cannot be neglected.

Upon UV irradiation, centered at the longer-wavelength absorption band, of Q2, Q3, and HI in nitrogen-saturated solutions, no formation of photoproducts of the starting materials was observed by spectrophotometric and NMR analysis (λ_{exc} corresponding to the longer-wavelength maximum). Therefore, the photoreaction described in the literature for these compounds has a quantum yield smaller than 0.001 under the present experimental conditions.[22]

The fluorescence properties of Q2, Q3, and HI were further investigated in acetonitrile and buffered solutions. The emission spectra of the three samples in ETN buffer are reported in Figure 1. For Q2 and Q3, the spectral features and the fluorescence quantum yields (ϕ_F) were not strongly affected by the solvent. The fluorescence lifetimes (τ_F) shown in Table 1 were measured both with the phase shift method and with the single photon counting technique. The trend of τ_F with the solvent is the same as that obtained for the fluorescence quantum yield, and the rate constants for the fluorescence decays are quite constant (Table 1) for Q2 and Q3 (2.3×10^7 and 7.7×10^7 s^{-1} in ETN, respectively) indicating that the $S_1 \rightarrow S_0$ transition is allowed and the nature of the S_1 state does not change with the nature of the medium.

The fluorescence spectrum of HI is solvent dependent, as shown by its bathochromic shift with the increase in the solvent polarity (Table 1). However, in the case of HI, the changes observed in the fluorescence properties are likely due to aggregates formation, as proven by the fluorescence measurements in less-polar solvents (data not shown).

Transient Properties. ***$T_1 \rightarrow T_n$ Absorption.*** Laser flash photolysis experiments ($\lambda_{exc} = 355$ nm) of the quinolizinium salts Q2, Q3, and HI in acetonitrile and in buffered solution at pH 7.2 (ETN) were carried out to obtain information on the transient behavior. The direct excitation of the three compounds led to a transient signal with maxima dependent on the compound and on the solvent (Table 2). In particular, the time-resolved

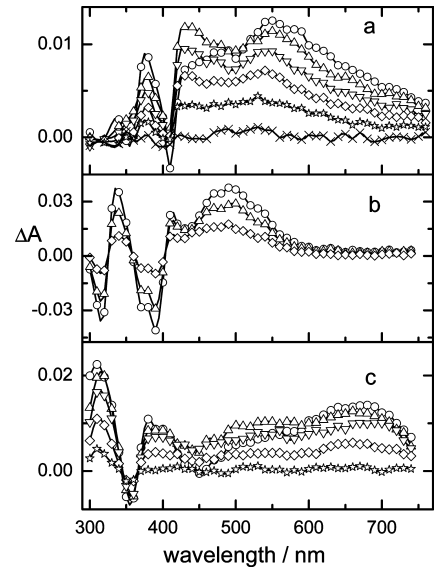

Figure 2. Time-resolved absorption spectra of (a) Q2 recorded 0.2 (○), 0.9 (△), 1.9 (▽), 3.0 (◇), 5.0 (☆), and 16 (×) μs after the laser pulse; (b) Q3 recorded 1.4 (○), 5.0 (△), and 16 (◇) μs after the laser pulse; and (c) HI recorded 0.4 (○), 1.3(△), 2.4 (▽), 4.0 (◇), and 6.0 (☆) μs after the laser pulse in ETN ($\lambda_{exc} = 355$ nm).

absorption spectra of Q2, Q3, and HI in ETN are shown in Figure 2 and present a maximum in the visible region ($\lambda_{max} =$ 490−690 nm) and one in the 320−380 nm range; in the region of 300−400 nm, the contribution of the ground state led to negative absorptions. In all cases, the kinetic analysis at different wavelengths revealed that the signal is due to only one transient, which is produced within the laser pulse and decays with a lifetime of few microseconds (Table 2), and the signal goes back to zero absorption values at long delay times. For all three compounds, the transient observed was assigned to the lowest excited triplet state T_1 because (i) it is formed within the laser pulse, (ii) its decay follows first-order kinetic, (iii) it is quenched by molecular oxygen at a diffusional limit, and (iv) it is sensitized by benzophenone, a well-known triplet energy donor.[15] The lifetime value of the T_1 state for Q2 and Q3 does not show a significant dependency on the solvent. The absence of residual absorption after the decay of the triplet state indicates that no other metastable species or photoproducts are formed upon laser irradiation under anaerobic conditions.

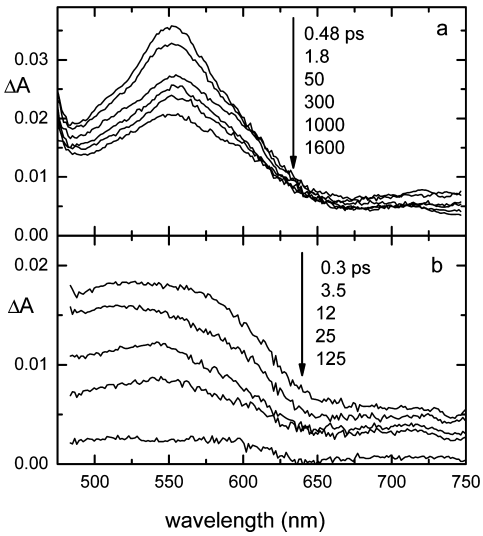

Figure 3. Time-resolved absorption spectra of Q2 in (A) the absence and (B) the presence of DNA ([DNA]/[Q2] = 21) recorded after the laser excitation at 400 nm.

The triplet absorption coefficients of Q2, Q3, and HI, expressed as a difference between the absorption coefficient of the triplet and the ground state ($\Delta\varepsilon_T$), were determined through the energy transfer method using benzophenone and disulphate benzophenone as sensitizers in acetonitrile and in aqueous solutions, respectively.[10,15] The $\Delta\varepsilon_T$ values range from 4400 to 5800 M^{-1} cm^{-1}, and they do not significantly depend on the solvent. Upon calibration of the instrumental set up with benzophenone in MeCN ($\phi_T \times \Delta\varepsilon_T = 6500$ M^{-1} cm^{-1} at 520 nm)[15] and using the measured $\Delta\varepsilon_T$ values, the triplet quantum yields of the compounds under investigation were determined (Table 2). For all compounds, the ϕ_T values are substantial (0.3 to 0.5) and are not significantly affected by the solvent.

Considering the determined fluorescence, ISC and reaction quantum yields make it clear that IC cannot be neglected in the deactivation of S_1 state (Table 1).

The triplet state of quinolizinium salts is quenched by molecular oxygen with the diffusion-controlled rate constant (k_{ox}) shown in Table 2. In acetonitrile, the quenching of the triplet state was accompanied by the formation of singlet oxygen, $O_2(^1\Delta_g)$, as proven by the presence of the singlet oxygen IR-luminescence detected upon excitation of the quinolizinium salts in air-equilibrated solutions. No luminescence was observed in the absence of substrate or by bubbling argon. The luminescence decay was described by a first-order kinetics with a lifetime very close to that reported in the literature.[23] The quantum yields for singlet oxygen production (ϕ_Δ) in MeCN were determined by the use of phenalenone as reference.[19] The ϕ_Δ values (ranging between 0.40 and 0.48) are slightly larger than the triplet yields; in fact, the longer the fluorescence lifetime, the larger the difference between ϕ_Δ and ϕ_T. The experimental errors do not allow us to state if the lowest singlet state is partially involved in the singlet oxygen formation. The short lifetime prevented the detection of singlet oxygen in aqueous solutions with the experimental setup at disposal.

Femtosecond Absorption. Femtosecond transient absorption spectra of Q2 and Q3 in ETN buffer (Figure 3a as an example) and MeCN were recorded by using 40 fs visible pump pulses centered at 400 nm and were simultaneously probed in the 470−780 nm range. HI could not be investigated with this technique owing to the formation of aggregates at the concentration used for these measurements. Positive ΔA signals that appear within the laser pulse with a broadband centered at 550 nm and ascribable to excited state absorptions were detected for both samples.

TABLE 3: Decay Lifetimes and Preexponential Factors at the Absorption Maxima for Q2 and Q3 in ETN and MeCN

compound	solvent	λ_{max}/nm	τ/ps	A/%
Q3	ETN	<470, 570	1/42/4800	20/29/51
	MeCN	595	1/20/5600	26/18/56
Q2	ETN	550	40/7500	18/82
	MeCN	575	27/8000	15/85

The global analysis of the decays measured at all absorption wavelengths revealed the presence of three exponential components in both ETN and MeCN in the case of Q3 and two components in the case of Q2 (Table 3). In particular, Q3 shows a very short component of about 1 ps, whereas decay components of tenths (20−40) of picoseconds and thousands (4800−8000) of picoseconds were detected for both Q2 and Q3.

Time-Resolved Fluorescence. The fluorescence decays of Q2 and Q3 in buffered solutions and water were recorded at different wavelengths in the 450−600 nm range exciting at 400 nm. (See Figure 4, where the reconstructed time-resolved fluorescence spectra of Q3 in MeCN are shown in the inset as an example.) The decays detected at each wavelength were corrected for the spectral response function of the instrument and normalized using the steady-state spectrum, as described in the literature.[24]

The observed fluorescence decays were fitted with a function that is a sum of exponentials and includes the convolution of the excitation profile using a nonlinear least-squares fitting procedure.

The analysis of the decay traces for Q2 and Q3 in ETN and MeCN (Table 3) showed the presence of two components with the same lifetimes (within the experimental error) already obtained by absorption measurements. A further 1 ps component, not clearly detectable in the case of Q2, was observed for Q3.

Even if an appropriate time-dependent Stokes shift analysis was prevented because the instrumental characteristics do not allow us to detect the whole Q3 emission band, the short-lived transient is likely assignable to the solvent rearrangement after Q3 excitation.[25,26] For Q2, the observation of this dynamic component is also prevented by the position of the fluorescence, which is blue-shifted compared with the one of Q3.

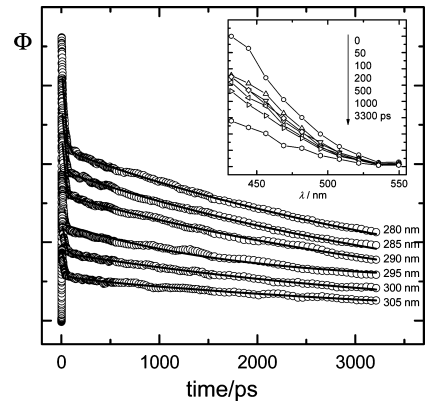

Figure 4. Upconverted fluorescence signal of Q3 in MeCN recorded at different emission wavelengths (λ_{exc}= 400 nm). Inset: fluorescence reconstructed spectra at different time delays.

A comparison between the longer-lived decay component of thousands of picoseconds and the fluorescence lifetime clearly allows us to assign this transient to the equilibrated excited singlet S_1 state of Q2 and Q3.

However, the decay components with decay time of 20−40 ps are likely assigned to the vibrational cooling of "hot" substrates in the excited state. Indeed, thermal equilibration, achieved through intramolecular vibrational energy redistribution and energy dissipation to the bath of solvent molecules, is known to occur within a few tens of picoseconds for many aromatic molecules in solution.[27−30]

Interactions of Quinolizinium Salts with DNA. ***Absorption and Emission Properties.*** Absorption spectra of quinolizinium salts in ETN buffer solution in the presence of an increasing amount of DNA (10^{-6} to 10^{-3} M) were recorded and analyzed according to the McGhee−von Hippel equation[31,32] to gain information on the properties of the substrate−DNA complexes in terms of association constant ($k_a \approx 1.5 \times 10^5$ M^{-1}) and occupational number ($n \approx 1$) under the present experimental conditions. The obtained results are in agreement with an intercalation model already reported in the literature, which shows that DNA is able to quench the steady-state fluorescence of the substrates without a significant change in the emission spectral shape.[3]

The fluorescence quantum yields analyzed with the Stern−Volmer equation allowed us to determine fluorescence quenching constants larger than the diffusional limit ($k_q \approx 10^{11}$ $M^{-1}s^{-1}$). Single photon counting measurements in the presence of increasing DNA concentrations did not reveal significant quenching in fluorescence decay times of Q2 and Q3, confirming that the interactions between DNA and quinolizinium salts are essentially in the ground state.

These experiments are in agreement with a static quenching of the singlet state in the binding site and the formation of an intercalation substrate−DNA complex that is essentially not fluorescent.

DNA Effect on the Transient of Quinolizinium Salts. Nanosecond laser flash photolysis experiments of quinolizinium salts were also carried out in the presence of DNA. The analysis of the recorded spectra and of the decay kinetics at different wavelengths allowed us to state that only one transient is formed within the laser pulse, and it decays with first-order kinetics.

The transient signal is assigned to the lowest triplet state of the dye because it has the same spectral and kinetic properties as the one observed without DNA; in particular, the addition of DNA does not modify the shape of the time-resolved spectra, but it significantly decreases the signal detected, and it increases the transient lifetime (Figure 5). These behaviors suggest that interactions with DNA inhibit the triplet state formation. The DNA concentration effects on τ_T (which are slight for Q2 and Q3) are likely due to changes in the ionic strength of the medium or in the concentration of molecular oxygen in the binding site; to clarify this point, further experimental study is needed.

Ultrafast 400 nm excitation of Q2 and Q3 in the presence of increasing amount of DNA produces time-resolved absorption spectra (Figure 3, panel B) and decay times of the primary transients that change with the concentration. The global analysis of the collected data and the best fit of the decay kinetics shows the presence of two components in all investigated systems whose time constants and relative weight depend on the [DNA]/[substrate] ratio. Figure 6 shows the normalized decay kinetics recorded at 520 nm for Q2; analogous results were obtained for Q3. These kinetic traces can be explained by taking into account the photon counting measurements and the behavior of pre-exponential factors upon the addition of DNA.

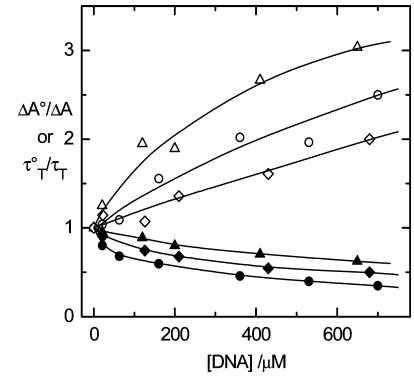

Figure 5. Effect of DNA concentration on the triplet absorption (open symbols) and triplet lifetime (full symbols) of Q2−30 μM (circles), Q3−30 μM (triangles), and HI (tilted squares) in ETN.

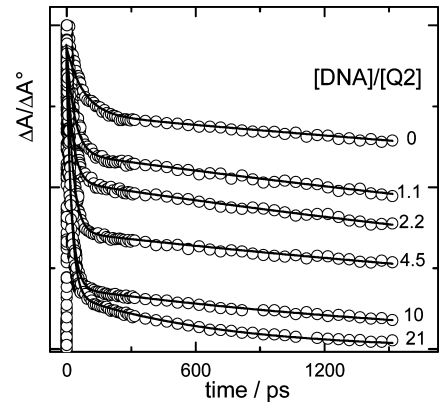

Figure 6. Normalized absorption decay traces of Q2 in ETN in the presence of different DNA concentrations recorded at 520 nm (λ_{exc} = 400 nm) at different time delays.

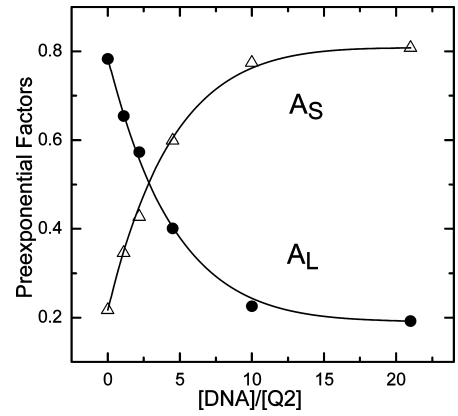

Figure 7. Pre-exponential factors of the short- and longer-lived components (A_S and A_L, respectively) of Q2 in the presence of different DNA concentrations (λ_{obsd} = 520 nm) obtained by the decay curves shown in Figure 6.

The effect of DNA concentration on the pre-exponential factors is also shown for Q2 in Figure 7; similar trends were obtained for Q3. In fact, the weight of the short-lived component increases markedly with DNA and becomes the most important one when the substrate interacts with the macromolecule.

The ultrafast absorption decays appear to be faster upon increasing DNA concentration because the contribution of the long component strongly decreases until it becomes almost negligible at high [DNA]/[Q] ratio. Table 4 shows the decay

TABLE 4: Time Constants of the Short-Lived Component (τ_S) of Q2 (λ_{obsd} = 520 nm) and Q3 (λ_{obsd} = 560 nm) in the Presence of Different DNA Concentrations in ETN (λ_{exc} = 400 nm)

[DNA]/[Q2]	τ_S/ps	[DNA]/[Q3]	τ_S/ps
0	42	0	40
1.1	34	0.7	32
2.2	29	1.3	26
4.5	27	2.9	24
10	24	5.9	16
21	22	14	10

times of the short-lived component, which decrease to values of 22 and 10 ps for Q2 and Q3, respectively.

The absorption spectra of the two components were obtained by global analysis at different [DNA]/[Q] ratios; Figure 8 shows the results obtained in the case of Q2. (A similar behavior was also obtained for Q3.) The full lines represent the absorption spectra of the longer-lived component, whose shape remains almost unchanged during DNA addition. On the contrary, the dashed lines, which represent the absorption spectra of the short-lived components, change significantly with DNA concentration; the shape becomes broader and slightly blue-shifted. At high [DNA]/[Q] ratios, where the longer-lived component almost disappears, the absorption maximum reaches a value of 535 and 500 nm for Q2 and Q3, respectively. On this basis, the decay times recorded at intermediate [DNA]/[Q] ratios (Table 4) reflect the relative weight of the free and complexed forms of Q2 and Q3 in solution.

These results allow us to assign the short-lived transient obtained in the presence of high DNA concentration to an excited singlet state of the substrate/DNA complex whose decay (in few tens of picoseconds) does not lead to new transient signals in the spectral window at disposal. Therefore, the fast decay is mainly due to nonradiative processes that likely involve energy dissipation from the intercalated substrate to the macromolecule. In fact, under our experimental conditions, neither triplet−triplet absorption nor fluorescence emission of the

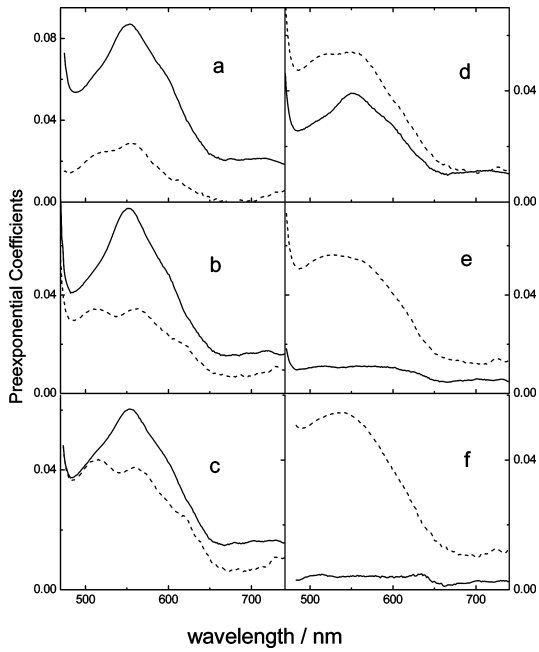

Figure 8. Absorption spectra of the short-lived (dashed lines) and longer-lived (full lines) components of Q2 at different [DNA]/[Q2] ratios: (a) 0, (b) 1.1, (c) 2.2, (d) 4.5, (e) 10, and (f) 21.

SCHEME 1: Chemical Structures of Investigated Compounds[a]

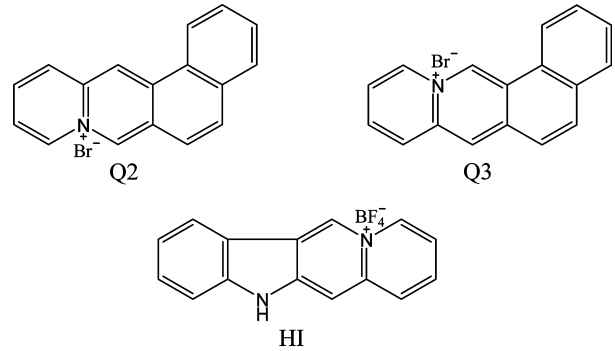

[a] Q2: naphto[1,2-*b*]quinolizinium bromide, Q3: naphto[2,1-*b*]quinolizinium bromide, HI: indolo[2,3-*b*]quinolizinium tetrafluoroborate.

substrate/DNA complex were observed; so that the major decay pathway of the complex excited state is likely an $S_1 \rightarrow S_0$ internal conversion process, followed by a vibrational relaxation of the ground state.

However, the broad absorption bands of the substrate/DNA complexes that resemble that of the guanine cation radical[33] could reflect the occurrence of charge-transfer interactions between the partners. According to these results, if a reactive channel was operative, then long-lived species detectable in the visible region would be likely formed by electron transfer from DNA to quinolizinium salts. Anyway, we cannot exclude the fact that this process occurred to such an extent that it did not produce a detectable concentration of the products.

The possibility of the formation of singlet oxygen seems to be ruled out by the particularly short-lived singlet complex.

Conclusions

The lowest singlet and triplet excited states of quinolizinium salts (HI, Q2, and Q3) were characterized in the absence and in the presence of DNA.

The S_1 state of the investigated compounds was characterized by absorption and emission spectroscopy and decays by fluorescence, $S_1 \rightarrow T_1$ intersystem crossing, and $S_1 \rightarrow S_0$ internal conversion with similar rate constants. The T_1 state is the only transient detected by nanosecond laser flash photolysis whose properties were not affected by the medium.

The investigated compounds are able to sensitize singlet molecular oxygen with quantum yields (ϕ_Δ = 0.40 to 0.48) that are slightly larger than the triplet quantum yields (ϕ_T = 0.30 to 0.43), but the experimental error does not allow us to state if the singlet state is also involved in the singlet oxygen sensitization process.

Ultrafast time-resolved measurements on Q2 and Q3 have shown, after solvent re-equilibration, the presence of two decay components. A short-lived component of a few tens of picoseconds was assigned to vibrational cooling, resulting from energy dissipation to the solvent, of the excited states reached upon 400 nm excitation. The longer-lived component with time constants in the nanosecond range was assigned to the decay of the relaxed S_1 state by comparison with the fluorescence lifetime.

To get information on the mechanism of DNA photocleavage induced by quinolizinium salts, the same investigations were carried out in the presence of DNA. In agreement with literature data,[3] steady-state measurements have shown that the substrates interact efficiently with DNA in the ground state to give intercalation complexes that are essentially not fluorescent.

Ultrafast absorption measurements on Q2 and Q3 allowed us to obtain the singlet−singlet absorption spectra of the substrate/DNA complexes together with their decay times of 22 (for DNA/Q2) and 10 ps (for DNA/Q3). Under these experimental conditions, no triplet absorption and fluorescence were detected, thus suggesting that the complexes likely decay by fast $S_1 \rightarrow S_0$ internal conversion, followed by energy dissipation through vibrational modes. These results cannot completely exclude the presence of a charge transfer process within the complexes involving the DNA base pairs, even with a low efficiency which does not allow accumulation of the intermediates responsible for DNA strand break; experiments are in progress to better clarify this point.

These detailed investigations suggest that the free dye molecules (present at the equilibrium) are responsible for the DNA photodamage, likely via singlet oxygen interactions.

Acknowledgment. We thank Dott. G. Viola (Padua, Italy) for the gifted samples. We gratefully acknowledge the financial support of the Ministero per l'Università e la Ricerca Scientifica e Tecnologica (Rome, Italy) and the University of Perugia.

References and Notes

(1) Ihmels, H.; Faulhaber, K.; Wissel, K.; Bringmann, G.; Messer, K.; Viola, G.; Vedaldi, D. *Eur. J. Org. Chem.* **2001**, 1157–1161.

(2) Viola, G.; Dall'Acqua, F.; Gabellini, N.; Moro, S.; Vedaldi, D.; Ihmels, H. *ChemBioChem* **2002**, *3*, 550–558.

(3) Viola, G.; Bressanini, M.; Gabellini, N.; Vedaldi, D.; Dall'Acqua, F.; Ihmels, H. *Photochem. Photobiol. Sci.* **2002**, *1*, 882–889.

(4) Ihmels, H.; Faulhaber, K.; Wissel, K.; Viola, G.; Vedaldi, D. *Org. Biomol. Chem.* **2003**, *1*, 2999–3001.

(5) Ihmels, H.; Faulhaber, K.; Vedaldi, D.; Dall'Acqua, F.; Viola, G. *Photochem. Photobiol.* **2005**, *81*, 1107–1115.

(6) Ihmels, H.; Otto, D.; Dall'Acqua, F.; Faccio, A.; Moro, S.; Viola, G. *J. Org. Chem.* **2006**, *71*, 8401–8411.

(7) Wagner, S. J.; Skripehenko, A.; Robinette, D.; Foley, J. W.; Cincotta, L. *Photochem. Photobiol.* **1998**, *67*, 343–349.

(8) Gupta, S. P. *Chem. Rev.* **1994**, *94*, 1507–1551.

(9) Bohne, C.; Faulhaber, K.; Giese, B.; Häfner, A.; Hofmann, A.; Ihmels, H.; Köhler, A. K.; Perä, S.; Schneider, F.; Sheepwash, M. A. L. *J. Am. Chem. Soc.* **2005**, *127*, 76–85.

(10) Favaro, G.; Romani, A. *J. Chem. Soc., Faraday Trans.* **1993**, *89*, 699–702.

(11) Eaton, D. F. In *Handbook of Organic Photochemistry*, Scaiano, J. C., Ed.; CRC Press: Boca Raton, FL, 1989; Vol. I, pp 231−239 and references therein.

(12) Beechem, J. M.; Gratton, E.; Ameloot, M.; Kutson, J. R.; Brand, L. In *Fluorescence Spectroscopy, Principles, and Techniques*, Lakowicz, J. R., Ed.; Plenum Press: New York, 1988; Vol. I and references therein.

(13) Görner, H.; Elisei, F.; Aloisi, G. G. *J. Chem. Soc., Faraday Trans.* **1992**, *88*, 29–34.

(14) Romani, A.; Elisei, F.; Masetti, F.; Favaro, G. *J. Chem. Soc., Faraday Trans.* **1992**, *88*, 2147–2154.

(15) Carmichael, I.; Hug, G. L. *J. Chem. Phys. Ref. Data* **1786**, *15*, 1–204.

(16) Fouassier, J. P.; Lougnot, D. J.; Zuchowics, I.; Green, P. N.; Timpe, H. J.; Kronfeld, K. P.; Müller, U. *J. Photochem.* **1987**, *36*, 347–363.

(17) Elisei, F.; Aloisi, G. G.; Lattarini, C.; Latterini, L.; Dall'Acqua, F.; Guiotto, A. *Photochem. Photobiol.* **1996**, *64*, 67–74.

(18) Becker, R. S.; Seixas de Melo, J.; Maçanita, A. L.; Elisei, F. *J. Phys. Chem.* **1996**, *100*, 18683–18695.

(19) Schmidt, R.; Tanielian, C.; Dunsbach, R.; Wolff, C. *J. Photochem. Photobiol., A: Chem.* **1994**, *79*, 11–17.

(20) Quillard, S.; Louarn, G.; Lefrant, S.; Macdiarmid, A. G. *Phys. Rev. B* **1994**, *50*, 496–508.

(21) Nakazono, M.; Nanbu, S.; Uesaki, A.; Kuwano, R.; Kashiwabara, M.; Zaitsu, K. *Org. Lett.* **2007**, *9*, 3583–3586.

(22) Ihmels, H.; Mohrschladt, C. J.; Schmitt, A.; Bressanini, M.; Leusser, D.; Stalke, D. *Eur. J. Org. Chem.* **2002**, *15*, 2624–2623.

(23) Adams, D. R.; Wilkinson, F. *J. Chem. Soc., Faraday Trans. 2* **1972**, *68*, 586–593.

(24) Karni, Y.; Jordens, S.; De Belder, G.; Schweitzer, G.; Hofkens, J.; Gensch, T.; Maus, M.; De Schryver, F. C.; Hermann, A.; Müllen, K. *Chem. Phys. Lett.* **1999**, *310*, 73–78.

(25) Nishiyama, K.; Hirata, F.; Okada, T. *Chem. Phys. Lett.* **2000**, *330*, 125–131.

(26) Glasbeek, M.; Zhang, H. *Chem. Rev.* **2004**, *104*, 1929–1954.

(27) Wang, H.; Zhang, H.; Abou-Zied, O. K.; Yu, C.; Romesberg, F. E.; Glasbeek, M. *Chem. Phys. Lett.* **2003**, *367*, 599–608.

(28) Zhong, D.; Douhal, A.; Zewail, A. H. *Proc. Natl. Acad. Sci. U.S.A.* **2000**, *97*, 14056–14061.

(29) Chou, P. T.; Chen, Y. C.; Yu, W. S.; Chou, Y. H.; Wei, C. Y.; Cheng, Y. M. *J. Phys. Chem. A* **2001**, *105*, 1731.

(30) Abou-Zied, O. K.; Jimenez, R.; Thompson, E. H. Z.; Millar, D. P.; Romesberg, F. E. *J. Phys. Chem. A* **2002**, *106*, 3665–3672.

(31) Schatchard, G. *Ann. N.Y. Acad. Sci.* **1949**, *51*, 660–672.

(32) McGhee, J. D.; von Hippel, P. H. *J. Mol. Biol.* **1974**, *86*, 469–489.

(33) Adhikarya, A.; Kumar, A.; Becker, D.; Sevilla, M. D. *J. Phys. Chem. B* **2006**, *110*, 24171–24180, and references therein cited.

JP9040315